

Structural Diversity in Neodymium Bipyrimidine Compounds with Near Infrared Luminescence: from Mono- and Binuclear Complexes to Metal-Organic Frameworks

Gaël Zucchi,^{*,†} Olivier Maury,[‡] Pierre Thuéry,[†] and Michel Ephritikhine[†]

CEA, IRAMIS, SCM, Laboratoire Claude Fréjacques, CNRS URA 331, 91191 Gif-sur-Yvette, France, and Laboratoire de Chimie, UMR 5182 CNRS-ENS Lyon, 46 allée d'Italie, 69364 Lyon Cedex 07, France

Received May 28, 2008

Treatment of $\text{Nd}(\text{NO}_3)_3$ with 2,2'-bipyrimidine (bpm) afforded the mononuclear adduct $[\text{Nd}(\text{NO}_3)_3(\text{bpm})(\text{MeOH})_2]$ (**1**) after recrystallization from MeOH, while reactions of hydrated NdCl_3 and various β -diketonates in the presence of bpm gave the binuclear compounds $[\{\text{Nd}(\text{dbm})_3(\text{THF})_2(\mu\text{-bpm})\}]$ (**2**) and $[\{\text{Nd}(\text{hta})_3(\text{MeOH})_2(\mu\text{-bpm})\} \cdot \text{bpm}]$ (**3** · bpm) (Hdbm = dibenzoylmethane, Hhta = 4,4,4-trifluoro-1-phenyl-1,3-butanedione) and the one-dimensional coordination polymer $[\text{Nd}(\text{tta})_3(\mu\text{-bpm}) \cdot \text{MeOH}]_\infty$ (**4** · MeOH) (Htta = 2-thenoyltrifluoroacetone). The crystal structures of **2–4** demonstrate that the bpm molecule can act as a planar bridging ligand between two lanthanide ions as large as Nd^{3+} . Luminescence measurements revealed that near-IR emission from neodymium can be obtained after excitation of either the bpm or the β -diketonate ligand, and that an energy transfer occurs from the β -diketonate group to the bpm molecule.

Introduction

Much attention is currently paid to materials incorporating lanthanide ions which, in view of their flexible coordination geometry and unique optical and magnetic features, are quite appropriate for engineering solids with tunable structural and physical properties. Lanthanide-based systems find applications as light emitters,^{1–4} (photo)catalysts,^{5–7} and magnetic materials.^{8,9} Regarding emission properties, the huge interest devoted to lanthanide ions is due to their extremely narrow

emission bands combined with relatively long excited-state lifetimes that result from intraconfigurational 4f-4f transitions. In addition, the color of the emission can easily be tuned from the UV to the near-infrared (NIR) region of the electromagnetic spectrum by a proper choice of the metal ion.¹⁰ Luminescence in the NIR is of interest for medical applications, as biological tissues are transparent in this spectral range,¹¹ or for telecommunications. In particular, materials incorporating Nd^{3+} and Er^{3+} ions are well-suited because their emission lines are relevant to the telecommunication window at 1.34 and 1.54 μm , respectively; thus, they are used for optical amplification for integrated optics,^{12–14} and Nd^{3+} is widely employed in solid-state lasers.¹⁵ It has also been demonstrated that these IR-emitters have a great potential in photonic devices such as light-emitting diodes.^{12,16–20}

* To whom correspondence should be addressed. E-mail: gael.zucchi@cea.fr.

[†] CEA.

[‡] ENS Lyon.

- (1) Bünzli, J.-C. G.; Piguet, C. *Chem. Soc. Rev.* **2005**, *34*, 1048.
- (2) Maas, H.; Curao, A.; Calzaferri, G. *Angew. Chem., Int. Ed.* **2002**, *41*, 2495.
- (3) Rocha, J.; Carlos, L. D. *Curr. Opin. Solid State Mater. Sci.* **2003**, *7*, 199.
- (4) Klönkowski, A. M.; Lis, S.; Pietraszkiewicz, M.; Hnatejko, Z.; Czarnobaj, K.; Elbanowski, M. *Chem. Mater.* **2003**, *15*, 656.
- (5) Cascales, C.; Lor, B. G.; Puebla, E. G.; Iglesias, M.; Monge, M. A.; Valero, C. R.; Snejko, N. *Chem. Mater.* **2004**, *16*, 4144.
- (6) Lin, W. B. *Mater. Res. Sci. Bull.* **2007**, *32*, 544.
- (7) Mahapatra, S.; Madras, G.; Row, T. N. G. *J. Phys. Chem. C* **2007**, *111*, 6505.
- (8) Benelli, C.; Gatteschi, D. *Chem. Rev.* **2002**, *102*, 2369.
- (9) Bonelli, L.; Sangregorio, C.; Sessoli, R.; Gatteschi, D. *Angew. Chem., Int. Ed.* **2005**, *44*, 5817.

(10) Hüstel, T.; Nikol, H.; Ronda, C. *Angew. Chem., Int. Ed.* **1998**, *37*, 3084.

(11) (a) Kim, S.; Lim, Y. T.; Soltesz, E. G.; De Grand, A. M.; Lee, J.; Nakayama, A.; Parker, J. A.; Mihaljevic, T.; Laurence, R. G.; Dor, D. M.; Cohn, L. H.; Bawendi, M. G.; Frangioni, J. V. *Nat. Biotechnol.* **2004**, *22*, 93. (b) Weissleder, R.; Ntziachristos, V. *Nat. Med.* **2003**, *9*, 123.

(12) Sloof, L. H.; van Blaaderen, A.; Polman, A.; Hebbink, G. A.; Klink, S. I.; van Veggel, F. C. J. M.; Reinhoudt, D. N.; Hofstraat, J. W. *J. Appl. Phys.* **2002**, *91*, 3955.

(13) Dignonet, M. J. F. *Rare Earth Doped Fiber Lasers and Amplifiers*, 2nd ed., Marcel Dekker Inc.: New York, 2001.

Among the materials investigated, coordination polymers with metal-organic frameworks have emerged as a new class with intriguing structural diversity and physical properties. Although lanthanides have often been regarded as unsuitable for the design of coordination polymers because of the lack of directional bonds making geometries difficult to predict and control, such hybrid materials have become a field of thorough investigations. Materials with unusual topologies²¹ such as three-dimensional porous solids^{22–25} or with unique luminescent or magnetic properties have been synthesized.^{26–28} The design and construction of such materials require a precise knowledge of the structure and behavior of the components, especially the key role of the organic linker in the structural assembly and the physicochemical properties. A number of lanthanide-based coordination polymers have been built up with a variety of carboxylic acids²² or anionic oxygen ligands such as phosphates and phosphonates.^{29–32} In contrast, molecules with nitrogen donors have been much less considered as associating ligands for the construction of metal organic frameworks with f-elements.^{33–35} In particular, 2,2'-bipyrimidine (bpm), whose numerous and various complexes of d transition metals have received great attention for their photocatalytic and magnetic

properties,^{36,37} is found in a relatively limited number of structurally characterized polynuclear lanthanide compounds: a few heterometallic 4f-d systems,^{38–40} the homobinuclear complexes $[\{(C_5Me_5)_2Eu\}_2(\mu\text{-bpm})]$,⁴¹ $[\{Ln(NO_3)_3(\mu\text{-bpm})\}_2(\mu\text{-bpm})]$ ($Ln = Eu, Tb$)⁴² and those of general formula $[\{Ln(\beta\text{-diketonate})_3\}_2(\mu\text{-bpm})]$ ($Ln = Eu, Tb$),^{43–47} and the one-dimensional arrays $[Ln(\text{hfac})_3(\mu\text{-bpm})]_\infty$ ($Ln = Eu$,⁴⁸ Gd, and Nd,⁴⁹ hfac = hexafluoroacetylacetonate). In the search of NIR luminescent neodymium complexes, we studied the systems composed of Nd^{3+} ions, bpm, and nitrate or β -diketonate ligands; these latter are commonly used as antenna ligands to overcome the low intensity of Laporte forbidden 4f-4f transitions, but their behavior in the presence of the bpm ligand has never been characterized. We have isolated a series of compounds showing diverse nuclearity and dimensionality, including a rare example of a structurally characterized mononuclear lanthanide complex with the bpm ligand, and of binuclear and one-dimensional polymeric compounds of a light lanthanide ensured by bridging bpm ligands. Here we present the synthesis and crystal structure of these complexes and their luminescent properties in the solid state.

Experimental Section

Materials and Methods. Reagents and solvents were purchased from Aldrich and used without further purification except the tetrahydrofuran (THF) used for the synthesis of **1** that was dried by standard methods and distilled before use. $[Nd(\text{dbm})_3(\text{H}_2\text{O})_2]$ was synthesized by a previously described synthetic procedure.⁵⁰ IR samples were prepared as KBr pellets, and the spectra were recorded with a Perkin-Elmer FTIR 1725X spectrometer. Elemental analyses were performed by Analytische Laboratorien at Lindlar (Germany).

Synthesis of $[Nd(NO_3)_3(\text{bpm})(\text{MeOH})_2]$ (1**).** A 50 mL round-bottom flask was charged with bpm (292 mg, 1.80 mmol) and $Nd(NO_3)_3 \cdot 6\text{H}_2\text{O}$ (609 mg, 1.8 mmol), and THF (10 mL) was condensed in it. After stirring for 1 h at room temperature, the white

(14) Reisfeld, R.; Jorgensen, C. K. *Lasers and Excited States of Rare Earths*; Springer: Berlin, 1977.

(15) Vieira, N. D., Jr.; Ranieri, I. M.; Tarelho, L. V. G.; Wetter, N. U.; Baldochi, S. L.; Gomes, L.; de Matos, P. S. F.; de Rossi, W.; Nogueira, G. E. C.; Courrol, L. C.; Barbosa, E. A.; Maldonado, E. P.; Morato, S. P. *J. Alloys Compd.* **2002**, *344*, 231.

(16) Sun, R. G.; Wang, Y. Z.; Zheng, Q. B.; Zhang, H. J.; Epstein, A. J. *J. Appl. Phys.* **2000**, *87*, 7589.

(17) Slooff, L. H.; Polman, A.; Cacialli, F.; Friend, R. H.; Hebbink, G. A.; van Veggel, F. C. J. M.; Reinhoudt, D. N. *Appl. Phys. Lett.* **2001**, *78*, 2122.

(18) Harrison, B. S.; Foley, T. J.; Knefely, A. S.; Mwaura, J. K.; Cunningham, G. B.; Kang, T.-S.; Bouguettaya, M.; Boncella, J. M.; Reynolds, J. R.; Schanze, K. S. *Chem. Mater.* **2004**, *16*, 2938.

(19) Harrison, B. S.; Foley, T. J.; Bouguettaya, M.; Boncella, J. M.; Reynolds, J. R.; Schanze, K. S.; Shim, J.; Holloway, P. H.; Padmanaban, G.; Ramakrishnan, S. *Appl. Phys. Lett.* **2001**, *79*, 3770.

(20) Suzuki, H. *J. Photochem. Photobiol. A* **2004**, *166*, 155.

(21) Hill, R. J.; Long, D.-L.; Hubberstey, P.; Schröder, M.; Champness, N. R. *J. Solid State Chem.* **2005**, *178*, 2414.

(22) Daiguebonne, C.; Kerbellec, N.; Bernot, K.; Deluzet, A.; Guillou, O. *Inorg. Chem.* **2006**, *45*, 5399.

(23) Pan, L.; Huang, X.; Li, J.; Wu, Y.; Zheng, N. *Angew. Chem., Int. Ed.* **2000**, *39*, 527.

(24) Serpaggi, F.; Luxbacher, T.; Cheetham, A. K.; Férey, G. J. *Solid State Chem.* **1999**, *145*, 580.

(25) Reineke, T. M.; Eddaoudi, M.; Fehr, M.; Kelley, D.; Yaghi, O. M. *J. Am. Chem. Soc.* **1999**, *121*, 1651.

(26) Thirumurugan, A.; Pati, S. K.; Green, M. A.; Natarajan, S. *J. Mater. Chem.* **2003**, *13*, 2937.

(27) Yang, J.; Yue, Q.; Li, G.-D.; Cao, J.-J.; Li, G.-H.; Chen, J.-S. *Inorg. Chem.* **2006**, *45*, 2857.

(28) Xia, J.; Zhao, B.; Wang, H.-S.; Shi, W.; Ma, Y.; Song, H.-B.; Cheng, P.; Liao, D.-Z.; Yan, S.-P. *Inorg. Chem.* **2007**, *46*, 3450.

(29) Guillou, O.; Daiguebonne, C. Lanthanide-containing Coordination Polymers. In *Handbook on the Physics and Chemistry of Rare Earths*; Gschneider, K. A.; Bünzli, J.-C. G.; Pecharsky, V. K., Eds.; Elsevier B. V.: New York, 2005; Vol. 34; pp 359–404.

(30) Cunha-Silva, L.; Mafra, L.; Ananias, D.; Carlos, L. D.; Rocha, J.; Almeida Paz, F. A. *Chem. Mater.* **2007**, *19*, 3527.

(31) Ngo, H. L.; Lin, W. *J. Am. Chem. Soc.* **2002**, *124*, 14298.

(32) Serpaggi, F.; Férey, G. *J. Mater. Chem.* **1998**, *8*, 2749.

(33) Müller-Buschbaum, K.; Mokaddem, Y. *Chem. Commun.* **2006**, 2060.

(34) Müller-Buschbaum, K.; Mokaddem, Y.; Schappacher, F. M.; Pöttgen, R. *Angew. Chem., Int. Ed.* **2007**, *46*, 4385.

(35) Müller-Buschbaum, K.; Gomes-Torres, S.; Larsen, P.; Wickleder, C. *Chem. Mater.* **2007**, *19*, 655.

(36) Inagaki, A.; Yatsuda, S.; Edure, S.; Suzuki, A.; Takahashi, T.; Akita, M. *Inorg. Chem.* **2007**, *46*, 2432.

(37) Armentano, D.; de Munno, G.; Guerra, F.; Faus, J.; Lloret, F.; Julve, M. *Dalton Trans.* **2003**, 4626.

(38) Baca, S. G.; Adams, H.; Sykes, D.; Faulfner, S.; Ward, M. D. *Dalton Trans.* **2007**, 2419.

(39) Shavaleev, N. M.; Accorsi, G.; Virgili, D.; Bell, Z. R.; Lazarides, T.; Calogero, G.; Armaroli, N.; Ward, M. D. *Inorg. Chem.* **2005**, *44*, 61.

(40) Shavaleev, N. M.; Bell, Z. R.; Ward, M. D. *Dalton Trans.* **2002**, 3925.

(41) Berg, D. J.; Boncella, J. M.; Andersen, R. A. *Organometallics* **2002**, *21*, 4622.

(42) Bekiari, V.; Thiakou, K. A.; Raptopoulou, C. P.; Perlepes, S. P.; Lianos, P. *J. Lumin.* **2008**, *128*, 481.

(43) (a) Jang, H.; Shin, C. H.; Jung, B. J.; Kim, D. H.; Shim, H. K.; Do, Y. *Eur. J. Inorg. Chem.* **2006**, 718. (b) Swavey, S.; Krause, J. A.; Collins, D.; D'Cunha, D.; Fratini, A. *Polyhedron* **2008**, *27*, 1061.

(44) D'Cunha, D.; Collins, D.; Richards, G.; Vincent, G. S.; Swavey, S. *Inorg. Chem. Commun.* **2006**, *9*, 979.

(45) Sultan, R.; Gadamssetti, K.; Swavey, S. *Inorg. Chim. Acta* **2006**, *359*, 1233.

(46) Fernandes, J. A.; Sa Ferreira, R. A.; Pillinger, M.; Carlos, L. D.; Jepsen, J.; Hazell, A.; Ribeiro-Claro, P.; Gonçalves, I. S. *J. Lumin.* **2005**, *113*, 50.

(47) Kirschbaum, K.; Fratini, A.; Swavey, S. *Acta Crystallogr., Sect. C* **2006**, *62*, m186.

(48) Fratini, A.; Swavey, S. *Inorg. Chem. Commun.* **2007**, *10*, 636.

(49) Fratini, A.; Richards, G.; Larder, E.; Swavey, S. *Inorg. Chem.* **2008**, *47*, 1030.

(50) Melby, L. R.; Rose, N. J.; Abramson, E.; Caris, J. C. *J. Am. Chem. Soc.* **1964**, *86*, 5177.

Table 1. Crystal Data and Structure Refinement Details

	1•MeOH	2	3•bpm	4
empirical formula	C ₁₁ H ₁₈ N ₇ NdO ₁₂	C ₁₀₆ H ₈₈ N ₄ Nd ₂ O ₁₄	C ₇₈ H ₅₆ F ₁₈ N ₈ Nd ₂ O ₁₄	C ₃₂ H ₁₈ F ₉ N ₄ NdO ₆ S ₃
<i>M</i> (g mol ⁻¹)	584.56	1930.28	1959.79	965.92
cryst syst	monoclinic	monoclinic	triclinic	monoclinic
space group	<i>P</i> 2 ₁ / <i>n</i>	<i>P</i> 2 ₁ / <i>c</i>	<i>P</i> $\bar{1}$	<i>C</i> 2/ <i>c</i>
<i>a</i> (Å)	8.3511(7)	9.7576(5)	9.8931(4)	22.7458(14)
<i>b</i> (Å)	15.6224(9)	15.2085(9)	12.3048(7)	16.6276(10)
<i>c</i> (Å)	16.0769(13)	29.2564(14)	16.4237(10)	22.4826(15)
α (deg)	90	90	101.910(3)	90
β (deg)	105.005(4)	92.128(3)	103.016(3)	114.619(6)
γ (deg)	90	90	90.116(3)	90
<i>V</i> (Å ³)	2025.9(3)	4338.6(4)	1903.53(18)	7730.2(9)
<i>Z</i>	4	2	1	8
<i>D</i> _{calcd} (g cm ⁻³)	1.917	1.478	1.710	1.660
μ (Mo K α) (mm ⁻¹)	2.639	1.254	1.464	1.595
<i>F</i> (000)	1156	1968	974	3800
reflns collected	40482	93639	51768	72350
indep reflns	3840	8208	7203	7298
obsd reflns [<i>I</i> > 2 σ (<i>I</i>)]	3350	7101	6414	4765
<i>R</i> _{int}	0.028	0.022	0.076	0.057
params refined	283	568	542	496
<i>R</i> 1	0.025	0.022	0.033	0.055
<i>wR</i> 2	0.056	0.056	0.075	0.145
<i>S</i>	1.045	1.046	1.050	1.061
$\Delta\rho_{\min}$ (e Å ⁻³)	-0.86	-0.57	-1.25	-0.98
$\Delta\rho_{\max}$ (e Å ⁻³)	0.41	0.30	0.47	0.90

powder was filtered off, washed with THF (3 × 5 mL) and dried under vacuum. Crystallization from methanol gave light purple crystals of **1**•MeOH (480 mg, 48%). IR (KBr): 3460 cm⁻¹ (ν_{OH}); 1574 and 1560 cm⁻¹ ($\nu_{\text{c-c}}$ bpm); 1470, 1305, 1027 cm⁻¹ (ν_{NO}). The crystals were found to desolvate upon drying under vacuum to give a purple powder of **1**. Anal. Calcd for C₁₀H₁₄N₇O₁₁Nd: C, 21.74; H, 2.55; N, 17.35%. Found: C, 21.83; H, 2.67; N, 17.79%.

Synthesis of [{Nd(dbm)₃(THF)₂(μ -bpm)]₂ (2). A 50 mL round-bottom flask was charged with Hdbm (213 mg, 0.95 mmol) in ethanol (10 mL) and aqueous 1 M NaOH (0.95 mL) was added. The solution was stirred at room temperature for 15 min and bpm (50 mg, 0.32 mmol) in ethanol (10 mL) and NdCl₃•6H₂O (113 mg, 0.32 mmol) were successively added. A white precipitate immediately formed and after stirring for 1 h, it was filtered off. Greenish-yellow crystals of **2** were obtained by slow diffusion of pentane (10 mL) into a THF solution (5 mL) of the crude reaction product (252 mg, 41%, based on Nd). Anal. Calcd for C₁₀₆H₈₈N₄O₁₄Nd₂: C, 65.95; H, 4.59; N, 2.90%. Found: C, 65.46; H, 4.20; N, 2.97%. IR (KBr): 1595 cm⁻¹ ($\nu_{\text{c-o}}$); ($\nu_{\text{c-c}}$ bpm) not identifiable because of absorption of dbm.

Synthesis of [{Nd(bta)₃(MeOH)₂(μ -bpm)]₂•bpm (3•bpm). By following the same procedure as for the preparation of the dbm derivative, the binuclear bta compound was synthesized from NdCl₃•6H₂O (113 mg, 0.32 mmol), Hbta (205 mg, 0.95 mmol), aqueous 1 M NaOH (0.95 mL) and bpm (50 mg, 0.32 mmol). Recrystallization from methanol afforded pale purple crystals of **3**•bpm (210 mg, 33% based on Nd). Anal. Calcd for C₇₈H₅₆F₁₈N₈O₁₄Nd₂: C, 47.37; H, 2.85; N, 5.67%. Found: C, 47.57; H, 3.08; N, 5.68%. IR (KBr): 3460 cm⁻¹ (ν_{OH}); 1614 cm⁻¹ ($\nu_{\text{c-o}}$); 1580, 1575, 1561 cm⁻¹ ($\nu_{\text{c-c}}$ bpm).

Synthesis of [Nd(tta)₃(bpm)]₂ (4). By following the same procedure as for the preparation of **2** and **3**, the coordination polymer was synthesized from hexahydrated NdCl₃ (113 mg, 0.32 mmol), Htta (211 mg, 0.95 mmol), aqueous 1 M NaOH (0.95 mL) and bpm (50 mg, 0.32 mmol), and isolated as an off-white powder. Crystals of **4**•MeOH were grown from a saturated methanol solution (240 mg, 78%). Anal. Calcd for C₃₂H₁₈F₉N₄O₆S₃Nd: C, 39.42; H, 1.86; N, 5.75%. Found: C, 39.20; H, 2.09; N, 5.61%. IR (KBr): 1614 cm⁻¹ ($\nu_{\text{c-o}}$); 1575, 1560 cm⁻¹ ($\nu_{\text{c-c}}$ bpm). These data are consistent with the absence of methanol after drying under vacuum.

Synthesis of [Nd(nta)₃(bpm)]₂ (5). By following the same procedure as for the preparation of **2**, **3**, and **4**, the nta compound (Hnta = 4,4,4-trifluoro-1-(2-naphthyl)-1,3-butanedione) was synthesized from NdCl₃•6H₂O (113 mg, 0.32 mmol), Hnta (252 mg, 0.95 mmol), aqueous 1 M NaOH (0.95 mL), and bpm (50 mg, 0.32 mmol). Pale purple crystals were obtained by cooling a hot THF solution of the crude reaction product (305 mg, 88%). Anal. Calcd for C₅₀H₃₀F₉N₄O₆Nd: C, 54.25; H, 2.73; N, 5.06%. Found: C, 54.43; H, 2.96; N, 4.89%. IR (KBr): 1614 cm⁻¹ ($\nu_{\text{c-o}}$); 1570, 1559 cm⁻¹ ($\nu_{\text{c-c}}$ bpm).

Crystallographic Data Collection and Structure Determination. The data were collected at 100(2) K on a Nonius Kappa-CCD area detector diffractometer⁵¹ using graphite-monochromated Mo K α radiation (λ 0.71073 Å). The crystals were introduced in glass capillaries with a protecting “Paratone-N” oil (Hampton Research) coating. The unit cell parameters were determined from ten frames, then refined on all data. The data (combinations of φ - and ω -scans giving complete data sets up to $\theta = 25.7^\circ$) were processed with HKL2000.⁵² The structures were solved by direct methods (**1**•MeOH, **2** and **4**) or by Patterson map interpretation (**3**•bpm) with SHELXS-97, expanded by subsequent Fourier-difference synthesis, and refined by full-matrix least-squares on *F*² with SHELXL-97.⁵³ Absorption effects were corrected empirically with the program SCALEPACK.⁵² All non-hydrogen atoms were refined with anisotropic displacement parameters. The hydrogen atoms bound to oxygen atoms were found on Fourier-difference maps when present, and all the others were introduced at calculated positions. All were treated as riding atoms with a displacement parameter equal to 1.2 (OH, CH, CH₂) or 1.5 (CH₃) times that of the parent atom. Some voids in the structure of **4** indicate the presence of unresolved solvent molecules; the available volume amounts to approximately 90 Å³ per asymmetric unit (i.e., per Nd atom), and it may correspond to one methanol molecule (which was however not added to the crystal chemical formula). Crystal data and structure refinement parameters are given in Table 1. The

(51) *Kappa-CCD Software*; Nonius BV: Delft, The Netherlands, 1998.

(52) Otwinowski, Z.; Minor, W. *Methods Enzymol.* **1997**, *276*, 307.

(53) Sheldrick, G. M. *SHELXS-97 and SHELXL-97*; University of Göttingen: Göttingen, Germany, 1997.

Table 2. Selected Bond Lengths (Å) and Angles (deg) for Complex **1**·MeOH

Nd–N(1)	2.655(2)	Nd–N(2)	2.645(2)
Nd–O(1)	2.5256(18)	Nd–O(2)	2.5366(18)
Nd–O(4)	2.5047(18)	Nd–O(5)	2.557(2)
Nd–O(7)	2.5673(17)	Nd–O(8)	2.5737(19)
Nd–O(10)	2.4856(19)	Nd–O(11)	2.4855(18)
N(1)–Nd–N(2)	61.31(6)	O(1)–Nd–O(2)	50.67(6)
O(4)–Nd–O(5)	50.78(6)	O(7)–Nd–O(8)	49.72(5)

molecular plots were drawn with SHELXTL⁵⁴ and ORTEP-3/POV-Ray.⁵⁵

Luminescence Spectra. All measurements were performed on dried crystals after being crushed in a mortar. The luminescence spectra in the solid state and in solution were recorded on a Horiba-Jobin Yvon Fluorolog-3 spectrofluorimeter, equipped with a three slit double grating excitation and emission monochromator with dispersions of 2.1 nm/mm (1200 grooves/mm). The steady-state luminescence was excited by unpolarized light from a 450 W xenon CW lamp and detected at an angle of 90° for diluted solution measurements or at 22.5° for solid state measurements by a red-sensitive Hamamatsu R928 photomultiplier tube. Spectra were reference corrected for both the excitation source light intensity variation (lamp and grating) and the emission spectral response (detector and grating). Uncorrected near-infrared spectra were recorded using a liquid nitrogen cooled, solid indium/gallium/arsenide detector (850–1600 nm).

Absorption Spectra. Solid UV–vis and near-infrared spectra were recorded from Teflon cells with Suprasil 300 quartz windows, using a Perkin-Elmer Lambda 950 instrument and PE Winlab software.

Results and Discussion

Synthesis and Characterization of the Complexes. Treatment of Nd(NO₃)₃·6H₂O with 1 equiv of bpm in THF led to the precipitation of an off-white powder. Pale purple crystals of [Nd(NO₃)₃(bpm)(MeOH)₂]·MeOH (**1**·MeOH) were obtained by crystallization from methanol in 48% yield. After [Ln(NO₃)₃(bpm)]₂(μ-bpm) (Ln = Eu, Tb),⁴² **1** is a new lanthanide nitrate complex with a bpm ligand and also a rare example of a lanthanide complex with bpm as a terminal ligand. **1** and the recently reported [Tb(hfac)₃(bpm)(H₂O)] compound⁴⁹ are the only mononuclear lanthanide compounds comprising bpm to have been crystallographically characterized. A view of **1** is shown in Figure 1 and selected bond lengths and angles are listed in Table 2. The ten-coordinate metal is in a distorted bicapped square antiprismatic environment, the square bases defined by the N(2), O(1), O(4), O(11) and O(2), O(5), O(8), O(10) atoms, and the N(1) and O(7) atoms in capping positions. The average Nd–O(NO₃) of 2.54(2) Å is identical to that measured in [Nd(NO₃)₃(bipy)₂] (bipy = 2,2'-bipyridine);⁵⁶ these Nd–O distances are 0.08 Å larger than the average Eu–O distance measured in [{Eu(NO₃)₃(bpm)]₂(μ-bpm), reflecting the variation in the radii of the Nd³⁺ and Eu³⁺ ions.⁵⁷ The average Nd–N(bpm) and Nd–N(bipy) distances of 2.650(5)

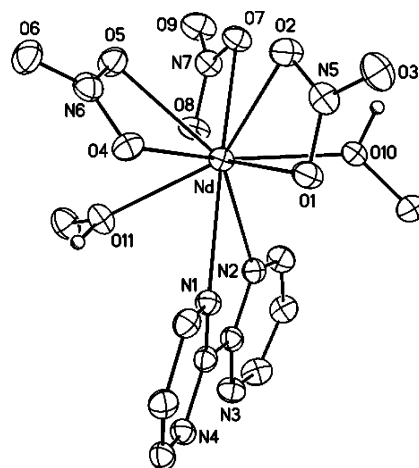


Figure 1. View of [Nd(NO₃)₃(bpm)(MeOH)₂] (**1**). Carbon-bound hydrogen atoms are omitted. Displacement ellipsoids are drawn at the 50% probability level.

and 2.60(1) Å are, respectively, 0.08 and 0.03 Å larger than the Eu–N distance corresponding to the terminal bpm ligand in the europium complex; the difference of 0.05 Å between the Nd–N(bpm) and Nd–N(bipy) distances could be related to the weaker Lewis basicity of the bpm versus bipy ligand.

The IR spectrum of **1** exhibits a strong absorption as a quasi-symmetric doublet at 1574 and 1560 cm⁻¹, diagnostic of a terminal chelating bpm ligand;^{58–60} the bands at 1470, 1305 and 1027 cm⁻¹ are characteristic of bidentate nitrate groups.^{42,61}

The synthesis of **1** is in contrast with that of the dinuclear complexes [{Ln(NO₃)₃(bpm)]₂(μ-bpm) (Ln = Eu, Tb) which were the only isolable products from the Ln(NO₃)₃·6H₂O/bpm reaction system, whatever the reagent ratio, the solvent, and the crystallization method used.⁴² Reaction of NdCl₃ with 3 equiv of dibenzoylmethane in a basic ethanolic solution and in the presence of 1 equiv of bpm immediately afforded a yellow precipitate which was dissolved in THF, and yellow greenish crystals of [{Nd(dbm)₃(THF)]₂(μ-bpm) (**2**) were obtained in 41% yield by slow diffusion of pentane into the solution. The centrosymmetric crystal structure of **2** is shown in Figure 2, and selected bond lengths and angles are listed in Table 3. The structure of complex **2** differs from that of the europium analogue [{Eu(dbm)₃]₂(μ-bpm)]⁴³ by the coordination of a supplementary THF molecule to the larger Nd³⁺ ion. The metal center is nine coordinate, in a distorted monocapped square antiprismatic configuration; the two square faces are defined by the O(1C), O(2A), O(2B), O(2C) and O(1), O(1A), O(1B), N(2') atoms and N(1) is in capping position. The Nd–N(1) and Nd–N(2') distances of 2.7611(16) and 2.7454(15) Å are 0.1 Å larger than those measured in the mononuclear complex **1**; such a difference was found between the Eu–N distances of the bridging and terminal bpm ligands in [{Eu(NO₃)₃(bpm)]₂(μ-bpm).⁴² The average

(54) Sheldrick, G. M. *SHELXTL*, version 5.1; Bruker AXS Inc.: Madison, WI, 1999.

(55) Farrugia, L. J. *J. Appl. Crystallogr.* **1997**, *30*, 565.

(56) Bower, J. F.; Cotton, S. A.; Fawcett, J.; Russell, D. R. *Acta Crystallogr., Sect. C* **2000**, *56*, e8.

(57) Shannon, R. D. *Acta Crystallogr., Sect. A* **1976**, *32*, 751.

(58) Bérézovsky, F.; Harem, A. A.; Triki, S.; Sala Pala, J.; Molinié, P. *Inorg. Chim. Acta* **1999**, *284*, 8.

(59) Hong, D. M.; Chu, Y. Y.; Wei, H. H. *Polyhedron* **1996**, *15*, 447.

(60) Julve, M.; Verdager, M.; De Munno, G.; Real, J. A.; Bruno, G. *Inorg. Chem.* **1993**, *32*, 795.

(61) Fawcett, J.; Platt, A. W. G.; Vickers, S.; Ward, M. D. *Polyhedron* **2004**, *23*, 2561.

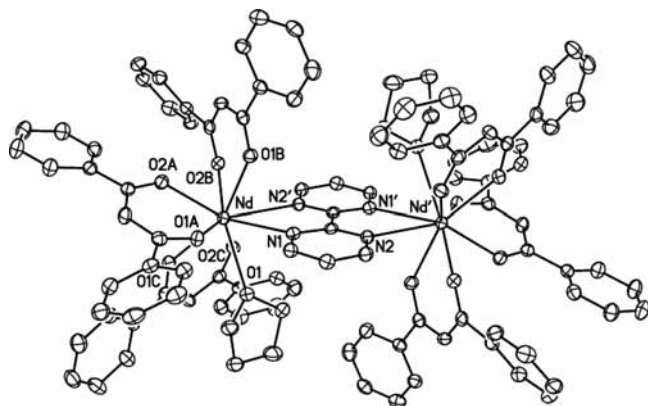


Figure 2. View of $[\{\text{Nd}(\text{dbm})_3(\text{THF})_2(\mu\text{-bpm})\}]_2$ (**2**). Hydrogen atoms are omitted. Displacement ellipsoids are drawn at the 50% probability level. Symmetry code: ' = $1 - x, 2 - y, -z$.

Table 3. Selected Bond Lengths (Å) and Angles (deg) for Complexes **2** and **3**·bpm^a

	2	3 ·bpm
Nd–N(1)	2.7611(16)	2.756(3)
Nd–N(2')	2.7454(15)	2.678(3)
Nd–O(1A)	2.4506(13)	2.4190(19)
Nd–O(2A)	2.3687(13)	2.4162(19)
Nd–O(1B)	2.4300(13)	2.4270(19)
Nd–O(2B)	2.4077(13)	2.4490(19)
Nd–O(1C)	2.3971(13)	2.467(2)
Nd–O(2C)	2.4879(13)	2.434(2)
Nd–O(1)	2.6322(13)	2.551(2)
N(1)–Nd–N(2')	58.74(4)	59.56(7)
O(1A)–Nd–O(2A)	70.70(4)	71.56(7)
O(1B)–Nd–O(2B)	71.20(4)	70.34(6)
O(1C)–Nd–O(2C)	69.45(4)	67.99(7)

^a Symmetry codes: ' = $1 - x, 2 - y, -z$ for complex **2**; ' = $1 - x, 1 - y, 1 - z$ for complex **3**.

Table 4. Selected Bond Lengths (Å) and Angles (deg) for Complex **4**^a

Nd–N(1)	2.769(5)	Nd–N(2')	2.808(5)
Nd–N(3)	2.803(5)	Nd–N(4'')	2.703(5)
Nd–O(1A)	2.453(5)	Nd–O(2A)	2.395(4)
Nd–O(1B)	2.439(4)	Nd–O(2B)	2.451(5)
Nd–O(1C)	2.446(5)	Nd–O(2C)	2.454(4)
N(1)–Nd–N(2')	57.72(14)	N(3)–Nd–N(4'')	58.43(14)
O(1A)–Nd–O(2A)	71.14(17)	O(1B)–Nd–O(2B)	68.96(14)
O(1C)–Nd–O(2C)	68.61(16)	N(2')–Nd–N(3)	171.23(15)

^a Symmetry codes: ' = $1 - x, 2 - y, 1 - z$; '' = $1/2 - x, 3/2 - y, 1 - z$.

Nd–O(dbm) distance of 2.42(4) Å can be compared with that of 2.39(2) Å in $[\text{Nd}(\text{dbm})_3(\text{phen})]$.⁶² The Nd···Nd' distance is 7.1831(3) Å.

Changing Hdbm with Hbta in its reaction with NdCl₃ in the presence of bpm led to the formation, after crystallization from methanol, of pale purple crystals of $[\{\text{Nd}(\text{bta})_3(\text{MeOH})\}_2(\mu\text{-bpm})] \cdot \text{bpm}$ (**3**·bpm). A view of **3**·bpm is shown in Figure 3 and selected bond lengths and angles are listed in Table 3. The Nd atom is here again in a distorted mono-capped square antiprismatic environment with N(1) in capping position. However, all three β-diketonate ligands labeled A–C (instead of two in **2**, labeled A and B) are spanning edges between the two square faces which are defined by the O(1), O(1C), O(2A), O(2B) and N(2'), O(1A),

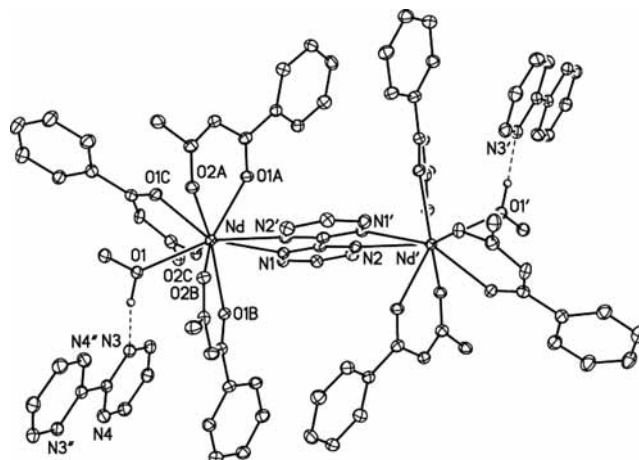


Figure 3. View of $[\{\text{Nd}(\text{bta})_3(\text{MeOH})_2(\mu\text{-bpm})\}]_2$ (**3**). Fluorine atoms and carbon-bound hydrogen atoms are omitted. Hydrogen bonds are shown as dashed lines. Displacement ellipsoids are drawn at the 30% probability level. Symmetry codes: ' = $1 - x, 1 - y, 1 - z$; '' = $2 - x, 1 - y, 2 - z$.

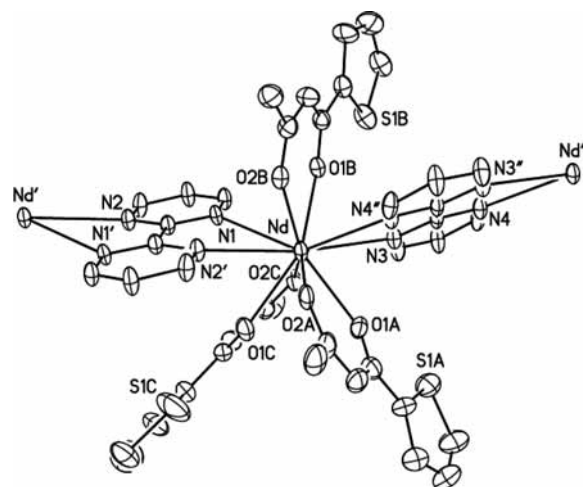


Figure 4. Partial view of $[\text{Nd}(\text{tta})_3(\mu\text{-bpm})]_\infty$ (**4**). Fluorine and hydrogen atoms are omitted. Displacement ellipsoids are drawn at the 20% probability level. Symmetry codes: ' = $1 - x, 2 - y, 1 - z$; '' = $1/2 - x, 3/2 - y, 1 - z$.

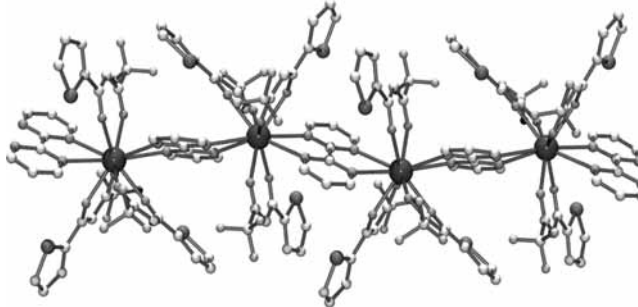


Figure 5. View of the polymeric arrangement in complex **4**. Hydrogen atoms are omitted. Atoms are represented as spheres of arbitrary radii.

O(2C), O(1B) atoms. The planar bpm ligand is not symmetrically chelated, the Nd–N(1) distance being 0.08 Å larger than Nd–N(2'). The average Nd–O(bta) distance of 2.435(18) Å is identical to the Nd–O(dbm) distance in **2**; the Nd···Nd' separation is 7.0885(5) Å.

Since the crystal structures of **2** and **3** demonstrated that the bpm molecule was capable of bridging Nd³⁺ ions in the presence of β-diketonates, the supposed mononuclear struc-

(62) Sun, L. N.; Zhang, H. J.; Meng, Q. G.; Liu, F. Y.; Fu, L. S.; Peng, C. H.; Yu, J. B.; Zheng, G. L.; Wang, S. B. *J. Phys. Chem. B* **2005**, *109*, 6174.

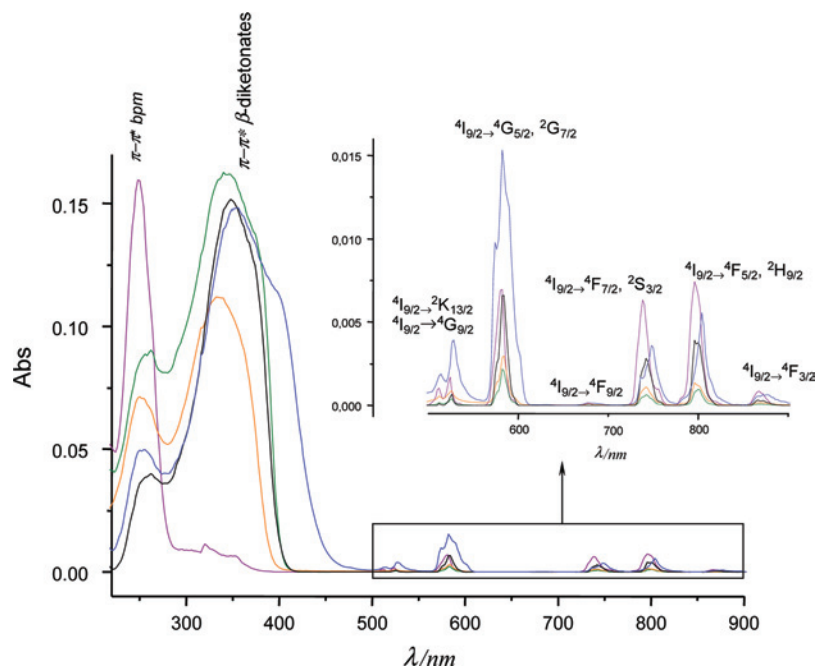


Figure 6. Solid state absorption spectra of **1** (purple), **2** (blue), **3** (orange), **4** (green), and **5** (black) (5% in MgO).

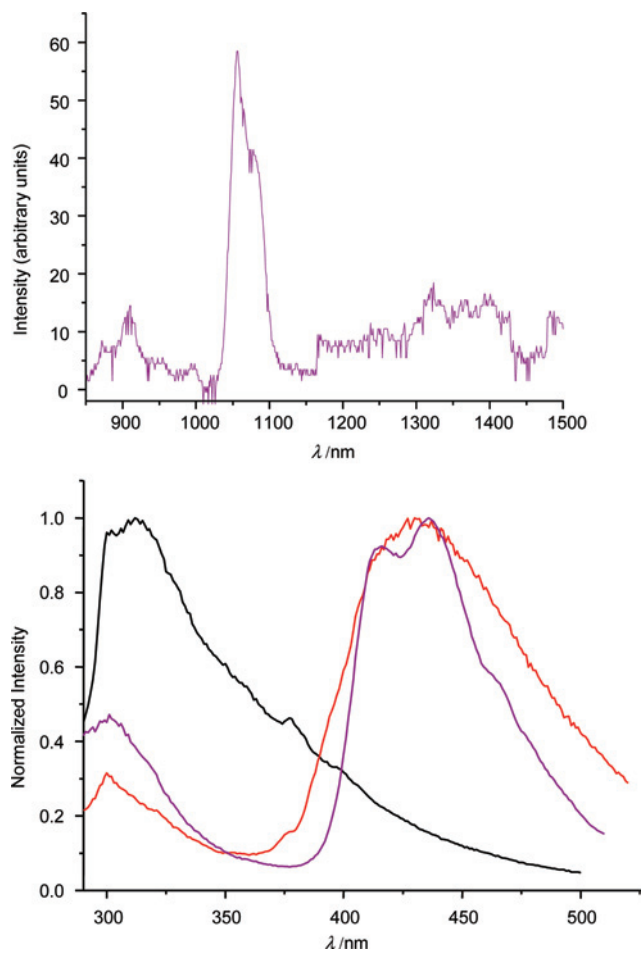


Figure 7. Top: emission spectrum of **1** in the near-IR ($\lambda_{\text{exc}} = 270$ nm); bottom: emission spectra in the UV–visible range ($\lambda_{\text{exc}} = 270$ nm) of **1** at 298 K in the solid state (purple) and in a DMF/MeOH (4:1) solution (black), and in frozen solution (red).

ture of $[\text{Nd}(\text{tta})_3(\text{bpm})]$ appeared questionable.^{44,45} Indeed, crystallization of this complex from methanol gave pale

purple crystals composed of polymeric chains of $[\text{Nd}(\text{tta})_3(\mu\text{-bpm})\cdot\text{MeOH}]_\infty$ (**4**·MeOH); views of **4** are shown in Figures 4 and 5 and selected bond lengths and angles are listed in Table 4. The metal center is in a distorted bicapped square antiprismatic environment, with the two square faces defined by the N(1), O(1C), O(2A), O(2B) and N(4''), O(1A), O(1B), O(2C) atoms, and N(2') and N(3) in capping positions. The average Nd–N and Nd–O distances of 2.77(4) and 2.44(2) Å, respectively, are quite similar to those measured in complexes **2** and **3**; these values can be compared with those of 2.70(3) and 2.44(6) Å in $[\text{Nd}(\text{tta})_3(\text{bipy})]$.⁶³

The IR spectrum of **4** exhibits a very asymmetric doublet at 1575 and 1560 cm^{-1} , characteristic of a bridging bpm ligand; this peak is masked in **2** by those of the dbm ligand. The IR spectrum of **3**·bpm shows, in addition to the absorption bands at 1575 and 1561 cm^{-1} , a peak at 1580 cm^{-1} corresponding to the free bpm molecule. From the IR spectrum (asymmetric doublet at 1570 and 1559 cm^{-1}), it is likely that the compound isolated as a white powder by using the β -diketone Hnta, the elemental analysis of which corresponds to the formula $[\text{Nd}(\text{nta})_3(\mu\text{-bpm})]$ (**5**), adopts a polymeric crystal structure similar to that of **4**, with bridging bpm ligands.

The distinct crystal structures of $[\{\text{Nd}(\text{dbm})_3(\text{THF})\}_2(\mu\text{-bpm})]$ (**2**) and $[\{\text{Eu}(\text{dbm})_3\}_2(\mu\text{-bpm})]$,⁴³ where the lanthanide ions are respectively nine- and eight-coordinate, can be accounted for by the larger size of the Nd^{3+} versus Eu^{3+} ion.⁵⁷ This explanation also holds for the comparison of the structures of $[\text{Nd}(\text{tta})_3(\mu\text{-bpm})\cdot\text{MeOH}]_\infty$ (**4**·MeOH) and $[\{\text{Eu}(\text{tta})_3\}_2(\mu\text{-bpm})]$,⁴³ where the metal centers are respectively ten- and eight-coordinate. It is noteworthy that the formation of the polymeric compound **4** is preferred to that of a binuclear complex of the type $[\{\text{Nd}(\text{tta})_3(\text{S})\}_2(\mu\text{-bpm})]$

(63) Leipoldt, J. G.; Bock, L. D. C.; Basson, S. S.; Laubscher, A. E. *J. Inorg. Nucl. Chem.* **1976**, *38*, 1477.

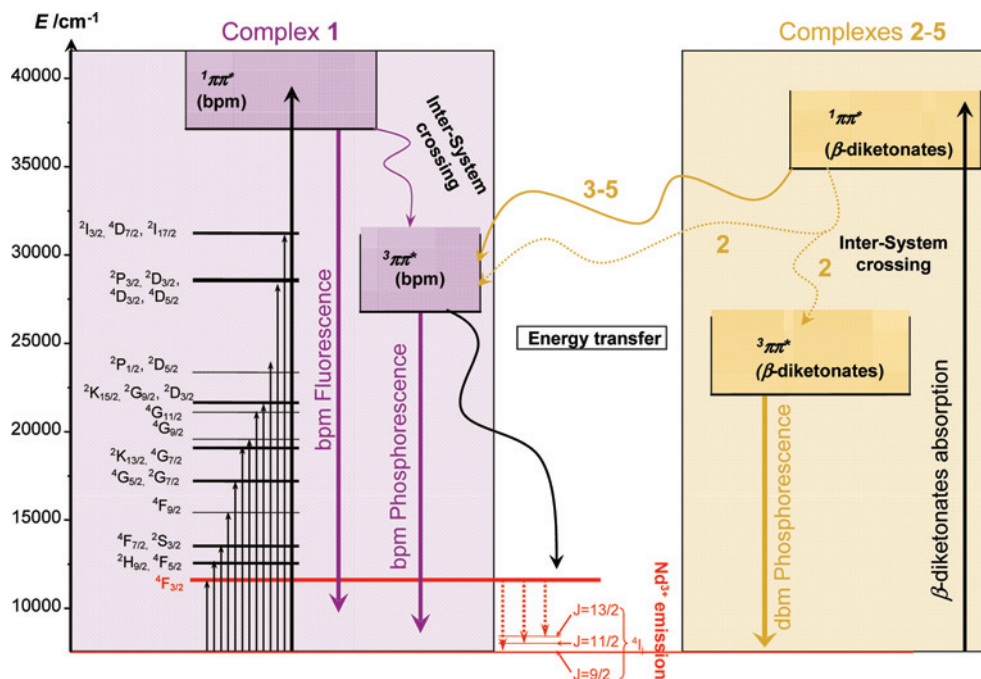


Figure 8. Energy level diagram for **1** in the solid state (left) and energy transfers occurring in **1–5**.

(S = solvent molecule), similar to **2** and **3**; the reasons for this difference are not obvious. The syntheses of the binuclear complex **2** and of the polymeric compound **4** (and presumably **5**), which are respectively nine and ten coordinate, are also in contrast with those of the mononuclear complexes $[\text{Nd}(\text{dbm})_3(\text{phen})]^{62}$ and $[\text{Nd}(\text{tta})_3(\text{bipy})]^{63}$; in these latter, the greater electron richness of the metal center, because of the more basic character and electron-donating capacity of bipy or phen than bpm, would impede the coordination of a supplementary ligand.

Photophysical Properties. The solid state absorption spectra of the compounds (5% in MgO) are shown in Figure 6. They all exhibit the typical parity-forbidden narrow absorption bands from the $^4\text{I}_{9/2}$ ground-state to various excited states of the Nd^{3+} ion and spin-allowed broad bands corresponding to π - π^* transitions within the electronic states of the ligands. These spectra clearly show the absorption bands of the bpm and β -diketonate ligands. The spectrum of **1** shows the absorption band due to bpm with a maximum at 249 nm. This band also appears for the other complexes, at 249 nm for **2** and **3** and at 262 nm for **4** and **5**. The β -diketonate ligands have absorption maxima at 354 nm (shoulder at 395 nm), 335 nm, 344 nm (shoulder at 366 nm), and 348 nm (shoulder at 372 nm) in **2**, **3**, **4**, and **5**, respectively.

When excited at 270 nm within a π - π^* transition of bpm, **1** shows the characteristic (although weak) narrow near-IR emission bands from the $^4\text{F}_{3/2}$ excited-state to the $^4\text{I}_J$ manifold with maxima at 910, 1061, and 1338 nm for $J = 9/2, 11/2,$ and $13/2$, respectively (Figure 7, top). This demonstrates that bpm can sensitize the Nd^{3+} luminescence in the near-IR. The spectrum also shows two bands which are due to emission from the first excited singlet (maximum at 300 nm) and triplet (structured band with maxima at 416 and 436 nm, and a shoulder at 460 nm) states of the bpm (Figure 7, bottom).

The assignment of the triplet emission has been established from variable temperature luminescence experiments in a 4:1 DMF: MeOH mixture. At room temperature, the emission spectrum shows only one broad band with a maximum at 310 nm, while the spectrum recorded at 77 K shows an emission band with a maximum at 431 nm which is similar to that observed in the solid state, in addition to the broad band centered at 300 nm. This assignment is further reinforced by the results we have obtained with the analogous terbium complex for which excitation at 270 nm afforded an intense terbium emission with no other emission band. Phosphorescence from the bpm is not observed for this complex; this indicates a relatively efficient energy transfer to the Tb(III) excited level.⁶⁴ These measurements definitely demonstrate that the broad band observed on the emission spectrum of **1** is due to the phosphorescence of bpm. The low efficiency of the bpm-to- Nd^{3+} energy transfer is explained by the difference in energy between the triplet state of the bpm and the $^4\text{F}_{3/2}$ excited-state of Nd^{3+} that is about 12000 cm^{-1} . This value is too high to afford an efficient energy transfer.⁶⁵ Furthermore, the relatively low emission intensity of the Nd(III) ion in this complex is also due to the presence of O–H oscillators in the first coordination sphere that efficiently quench the luminescence by a non-radiative energy transfer pathway. The data obtained above from absorption and emission measurements enable the establishment of the energy level diagram for **1** (Figure 8, left).

The emission spectra of complexes **2–5** in the visible and near-IR regions are shown in Figure 9. These spectra show well-structured near-IR emission bands of Nd^{3+} when excited at 260–270 nm within the bpm π - π^* bands, or after

(64) The results on the Tb(III) complex will be published elsewhere.

(65) Steemers, F. J.; Verboom, W.; Reinhoudt, D. N.; van der Tol, E. B.; Verhoeven, J. W. *J. Am. Chem. Soc.* **1995**, *117*, 9408.

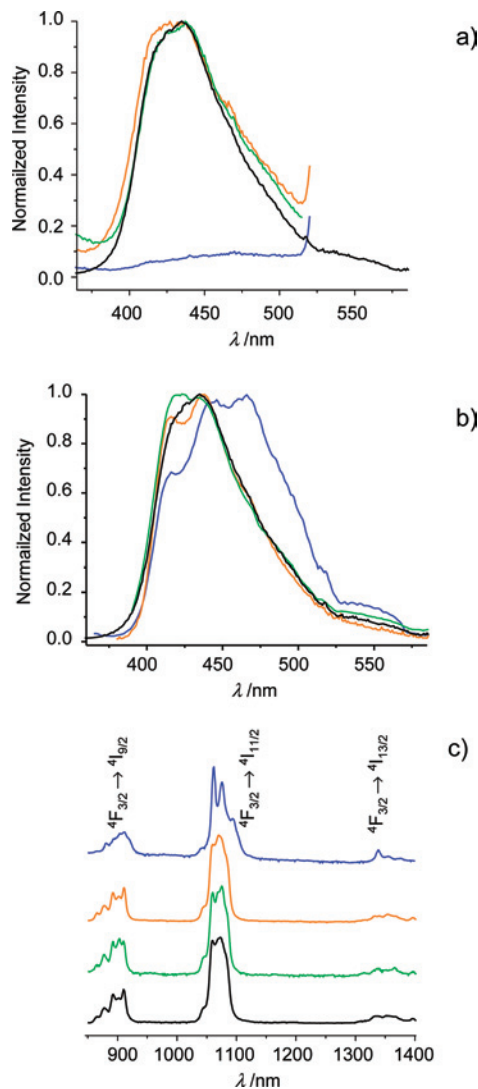


Figure 9. (a) Visible emission spectra of **2** (blue, $\lambda_{\text{exc}} = 270$ nm), **3** (orange, $\lambda_{\text{exc}} = 270$ nm), **4** (green, $\lambda_{\text{exc}} = 270$ nm), and **5** (black, $\lambda_{\text{exc}} = 260$ nm); (b) visible emission spectra of **2** (blue, $\lambda_{\text{exc}} = 353$ nm), **3** (orange, $\lambda_{\text{exc}} = 370$ nm), **4** (green, $\lambda_{\text{exc}} = 370$ nm), and **5** (black, $\lambda_{\text{exc}} = 333$ nm); (c) near-IR emission spectra of **2** (blue, $\lambda_{\text{exc}} = 370$ nm), **3** (orange, $\lambda_{\text{exc}} = 370$ nm), **4** (green, $\lambda_{\text{exc}} = 343$ nm), and **5** (black, $\lambda_{\text{exc}} = 370$ nm) in the solid state.

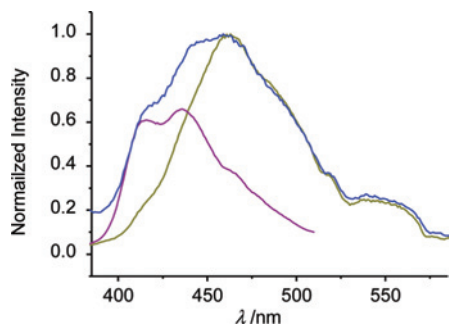


Figure 10. Normalized emission spectra of **1** (purple, $\lambda_{\text{exc}} = 270$ nm), **2** (blue, $\lambda_{\text{exc}} = 353$ nm), and $[\text{Nd}(\text{dbm})_3(\text{H}_2\text{O})_2]$ (dark green, $\lambda_{\text{exc}} = 353$ nm).

excitation within the β -diketonate π - π^* bands around 350 nm. Compounds **3–5** also exhibit broad emission bands between 370 and 580 nm with a similar envelope whatever the excitation wavelength used. This emission revealed that the bpm excited triplet state is populated when the β -dike-

tonate ligands are excited and reflects an energy transfer from the singlet state of the β -diketonates to the triplet state of bpm. As the emission of the triplet states of the dbm, bta, tta, and nta ligands of the $[\text{Ln}(\beta\text{-diketonate})_3(\text{H}_2\text{O})_2]$ complexes have been located at 490,^{66,67} 470,⁶⁸ 525,⁶⁹ and 571⁷⁰ nm, respectively, the β -diketonates-to-bpm energy transfer is made possible by the position of the triplet state of the bpm that lies at an energy localized in-between the excited levels of the β -diketonates (Figure 8, right). Complex **2** behaves in a different way since excitation of the dbm ligands at 353 nm results in a broad structured band between 380 and 570 nm. This band is due to phosphorescence from the bpm and dbm ligands, as shown in Figure 10 where we have reported the emission spectra of $[\text{Nd}(\text{dbm})_3(\text{H}_2\text{O})_2]$,^{66,67} **1**, and **2**. Thus, an energy transfer occurs from the dbm to the bpm, but it is not as efficient as it is for complexes **3–5**. Furthermore, excitation at 270 nm does not induce any phosphorescence from bpm. As yet, we have not been able to explain this different behavior experimentally observed for **2**. Finally, the dbm-bpm system is a better sensitizer than the hfac-bpm one for Nd^{3+} as luminescence from this ion in **2** has been detected in a methanol solution at room temperature, while no emission was observed for the hfac derivative⁴⁹ (Supporting Information).

Conclusion

We have described the X-ray crystal structures of four neodymium(III) complexes with bpm and nitrates or various β -diketonate ligands that are of interest for luminescence studies. These systems exhibit a remarkable structural diversity, as we have obtained one mononuclear and two dinuclear complexes and one coordination polymer by using identical synthetic procedures and stoichiometric quantities. They show that bpm can both act as a bridging or a terminal ligand in lanthanide chemistry. Investigation of the photophysical properties of compound **1** allowed the localization of the excited singlet and triplet states of bpm and demonstrated that this ligand could sensitize the Nd^{3+} luminescence in the near-IR. However, the $\text{Nd}(\text{III})$ emission intensity is low in **1** because of the poorly efficient energy transfer from bpm to the $^4\text{F}_{3/2}$ level and the presence of O–H oscillators in the first coordination sphere that deactivate the $\text{Nd}(\text{III})$ luminescence. In systems containing both bpm and β -diketonate ligands, an energy

(66) Hebbink, G. A.; Klink, S. I.; Oude Alink, P. G. B.; van Veggel, F. C. J. M. *Inorg. Chim. Acta* **2001**, *317*, 114.

(67) Yang, L.; Gong, Z.; Nie, D.; Lou, B.; Bian, Z.; Guan, M.; Huang, C.; Lee, H. J.; Baik, W. P. *New J. Chem.* **2006**, *30*, 791.

(68) Voloshin, A. I.; Shavaleev, N. M.; Kazalov, V. P. *J. Lumin.* **2000**, *91*, 49.

(69) Malta, O. L.; Brito, H. F.; Menezes, J. F. S.; Gonçalves e Silva, F. R.; Alves, S., Jr.; Farias, F. S., Jr.; de Andrade, A. V. M. *J. Lumin.* **1997**, *75*, 255.

(70) Carlo, L. D.; De Mello Donegá, C.; Albuquerque, R. Q.; Alves Jr, S.; Menezes, J. F. S.; Malta, O. L. *Mol. Phys.* **2003**, *101*, 1037.

(71) Banerjee, S.; Hueber, L.; Romanelli, M. D.; Kumar, G. A.; Riman, R. E.; Emge, T. J.; Brennan, J. G. *J. Am. Chem. Soc.* **2005**, *127*, 15900.

(72) Kumar, G. A.; Riman, R. E.; Diaz Torres, L. A.; Banerjee, S.; Romanelli, M. D.; Emge, T. J.; Brennan, J. G. *Chem. Mater.* **2007**, *19*, 2937.

(73) Romanelli, M.; Kumar, G. A.; Emge, T. J.; Riman, R. E.; Brennan, J. G. *Angew. Chem., Int. Ed.* **2008**, *47*, 6049.

transfer was found to occur between the β -diketonate and bpm ligands as phosphorescence from bpm is observed when the β -diketonate groups are excited. Thus, our work shows that the bpm ligand not only acts as a connector between neodymium ions but also plays an important role in the sensitization of the Nd(III) luminescence. Quantitative data on these luminescent systems need to be determined to further discuss their efficiency as near-IR emitters. To date, solid state studies of the luminescent properties of molecular neodymium complexes are relatively scarce. Some efficient systems involving chalcogenide clusters have been reported.^{71–73} It would be of

interest to draw a comparison between these latter and our systems.

Acknowledgment. We thank the CNRS and CEA for financial support.

Supporting Information Available: Figure with the emission spectrum of **2** in methanol (PDF). Tables of crystal data, atomic positions and displacement parameters, anisotropic displacement parameters, bond lengths and bond angles in CIF format. This material is available free of charge via the Internet at <http://pubs.acs.org>.

IC800967X